Study of e^+e^- annihilation into hadrons at low energies with ISR at BABAR

Peter A. Lukin

Budker Institute of Nuclear Physics and Novosibirsk State University, Novosibirsk, Russia

On behalf of BaBar Collaboration

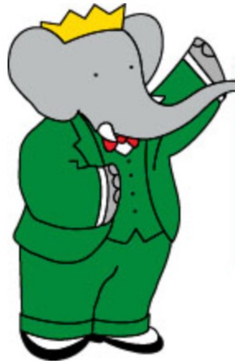

Outline

- New preliminary measurement of $e^+e^- \to \pi^+\pi^-\pi^0$ cross section
- First preliminary measurements of $e^+e^- \to \pi^+\pi^-4\pi^0$ and $e^+e^- \to \pi^+\pi^-3\pi^0\eta$ cross sections
- First measurements of $e^+e^- \to 2(\pi^+\pi^-)3\pi^0$ and $e^+e^- \to 2(\pi^+\pi^-)2\pi^0\eta$ cross sections

Phys.Rev.D 103, 092001 (2021)

BABAR hadronic cross section measurements using ISR

Initial State Radiation from e^+e^- allows to measure cross sections at all center-of-mass energies $\sqrt{s'}$ below the nominal $\sqrt{s}$ of the beams:

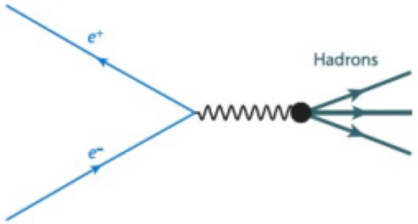

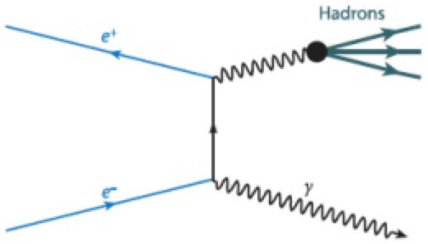

$$\frac{d\sigma(s;s';\theta_\gamma)}{ds'd\theta_\gamma} = W(s;s';\theta_\gamma) \cdot \sigma_X(s')$$

boost $\Longrightarrow$ harder momentum spectrum for daughter particles

- cross sections down to threshold
- measure σ at all $\sqrt{s}$ simultaneously
- large "effective" luminosity

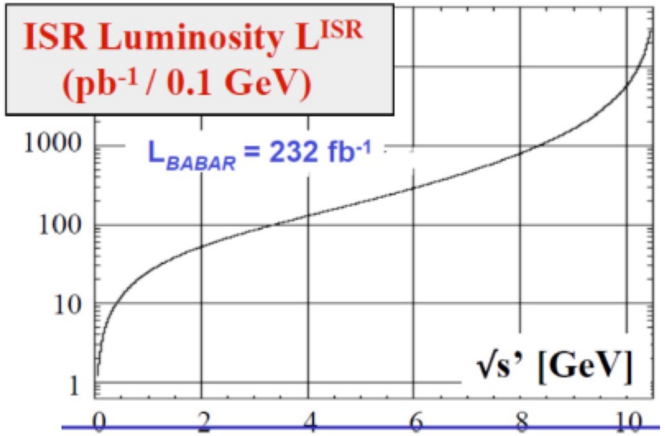

tag photon to identify ISR events

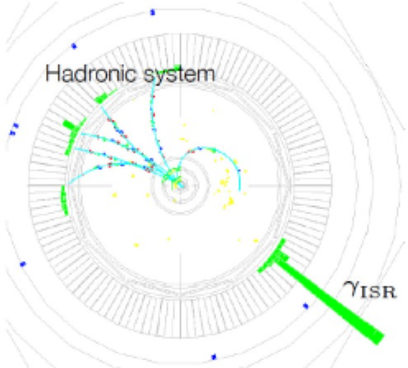

- hadrons in fiducial detector region
- fully reconstruct the final state
- kinematic fit: energy resolution

Light hadrons cross sections measured in ISR by BABAR

Many **first measurements**: (superseded results omitted)

$2(\pi^+\pi^-)\pi^0\pi^0\pi^0$ and $2(\pi^+\pi^-)\pi^0\pi^0\eta$	469 fb^{-1}	Phys. Rev. D 103, 092001 (2021)
$\pi^+\pi^-\pi^0\pi^0\pi^0$ and $\pi^+\pi^-\pi^0\pi^0\eta$	469 fb^{-1}	Phys. Rev. D 98, 112015 (2018)
$\pi^+\pi^-\eta$	469 fb^{-1}	Phys. Rev. D 97, 052007 (2018)
$\pi^+\pi^-\pi^0\pi^0$	454 fb^{-1}	Phys. Rev. D 96, 092009 (2017)
$K_S^0K^\pm\pi^\mp\pi^0$ and $K_S^0K^\pm\pi^\mp\eta$	454 fb^{-1}	Phys. Rev. D 95, 092005 (2017)
$K_S^0K_L^0\pi^0$, $K_S^0K_L^0\eta$, and $K_S^0K_L^0\pi^0\pi^0$	469 fb^{-1}	Phys. Rev. D 95, 052001 (2017)
K^+K^- (γ undetected)	469 fb^{-1}	Phys. Rev. D 92, 072008 (2015)
$K_S^0K_L^0$, $K_S^0K_L^0\pi^+\pi^-$, $K_S^0K_S^0\pi^+\pi^-$, and $K_S^0K_S^0K^+K^-$	469 fb^{-1}	Phys. Rev. D 89, 092002 (2014)
K^+K^-	232 fb^{-1}	Phys. Rev. D 88, 032013 (2013)
$p\bar{p}$	469 fb^{-1}	Phys. Rev. D 87, 092005 (2013)
$p\bar{p}$ (E_{cm} : 3.0 ÷ 6.5 GeV)	469 fb^{-1}	Phys. Rev. D 88, 072009 (2013)
$\pi^+\pi^-\pi^+\pi^-$	454 fb^{-1}	Phys. Rev. D 85, 112009 (2012)
$K^+K^-\pi^+\pi^-$, $K^+K^-\pi^0\pi^0$, and $K^+K^-K^+K^-$	454 fb^{-1}	Phys. Rev. D 86, 012008 (2012)
$\pi^+\pi^-$	232 fb^{-1}	Phys.Rev.Lett. 103, 231801 (2009)
$K^+K^-\eta$, $K^+K^-\pi^0$ and $K_s^0K^\pm\pi^\mp$	232 fb^{-1}	Phys. Rev. D 77, 092002 (2008)
$\Lambda\bar{\Lambda}$, $\Lambda\bar{\Sigma}^0$, and $\Sigma^0\bar{\Sigma}^0$	230, fb^{-1}	Phys. Rev. D 76, 092006 (2007)
$2(\pi^+\pi^-)\pi^0$, $2(\pi^+\pi^-)\eta$, $K^+K^-\pi^+\pi^-\pi^0$ and $K^+K^-\pi^+\pi^-\eta$	232 fb^{-1}	Phys. Rev. D 76, 092005 (2007)
$3(\pi^+\pi^-)$, $2(\pi^+\pi^-\pi^0)$ and $K^+K^-2(\pi^+\pi^-)$	232 fb^{-1}	Phys. Rev. D 73, 052003 (2006)
$\pi^+\pi^-\pi^0$	89 fb^{-1}	Phys. Rev. D 70, 072004 (2004)

$e^+e^- \to \pi^+\pi^-\pi^0$

It gives the second largest contribution to a_μ^{HLO} and its error

Abs. contr. to a_μ^{HLO}

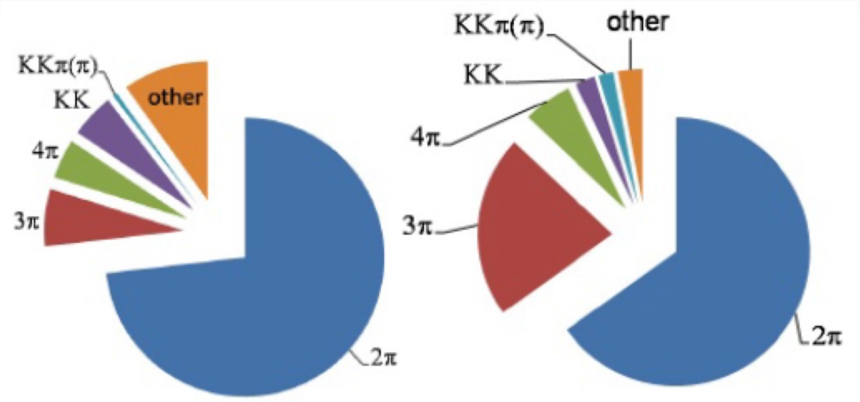

Error (squared) contr. a_μ^{HLO}

Previous *BABAR* measurement based on 1/5 of dataset

Cross section had been measured in $1.05 \div 3$ GeV

PRD 70, 072004 (2004)

New preliminary measurement using the whole dataset extends cross section below 1.05 GeV, in the region of ρ, ω and ϕ resonances

accuracy on a_μ^{HLO} contribution due to $e^+e^- \to \pi^+\pi^-\pi^0$ currently $\approx 3\%$

new measurement will improve accuracy to $\approx 1.5\%$

$e^+e^- \to \pi^+\pi^-\pi^0\gamma_{ISR}$

preliminary

Detect all final state particles

Select events using kinematic fit (cut on χ^2)

Several additional cuts reduce background by factor 2

Remaining ISR and $q\bar{q}$ background subtracted using simulation normalized to data.

Above 1.1 GeV sizeable FSR background from $e^+e^- \to a_1\gamma$, $a_2\gamma$ processes.

Estimated by pQCD with 100% uncertainty.

up to 8% contribution near 1.3 GeV

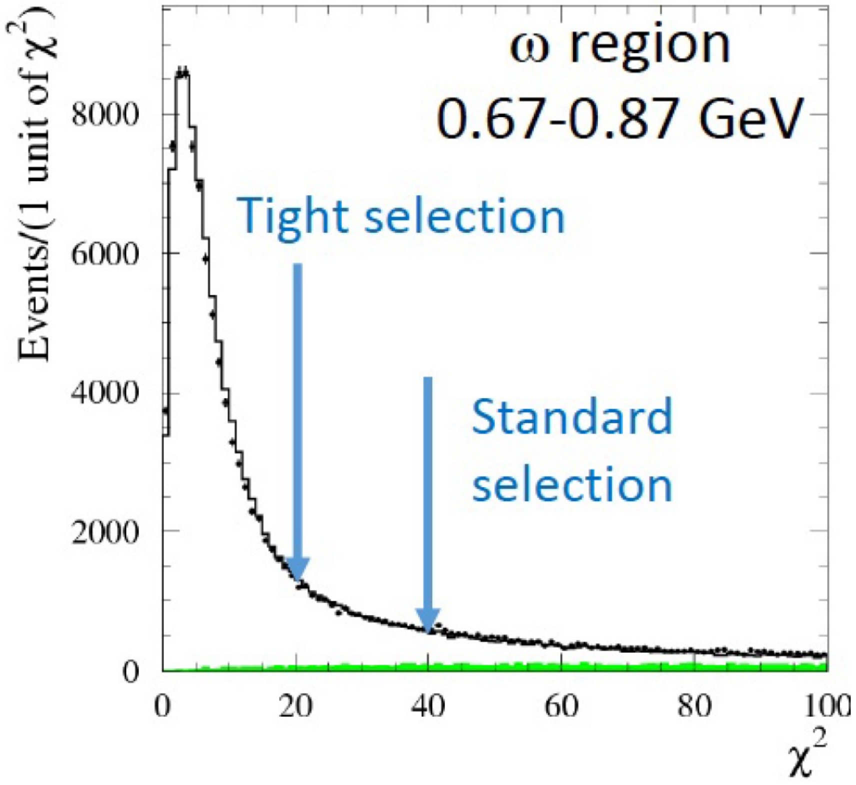

$\pi^+\pi^-\pi^0$ mass spectrum below 1.1 GeV

preliminary

Below 1.1 GeV the mass spectrum has a sharp structure

unfolding required to determine true spectrum

cross section result depends on the assumed mass resolution

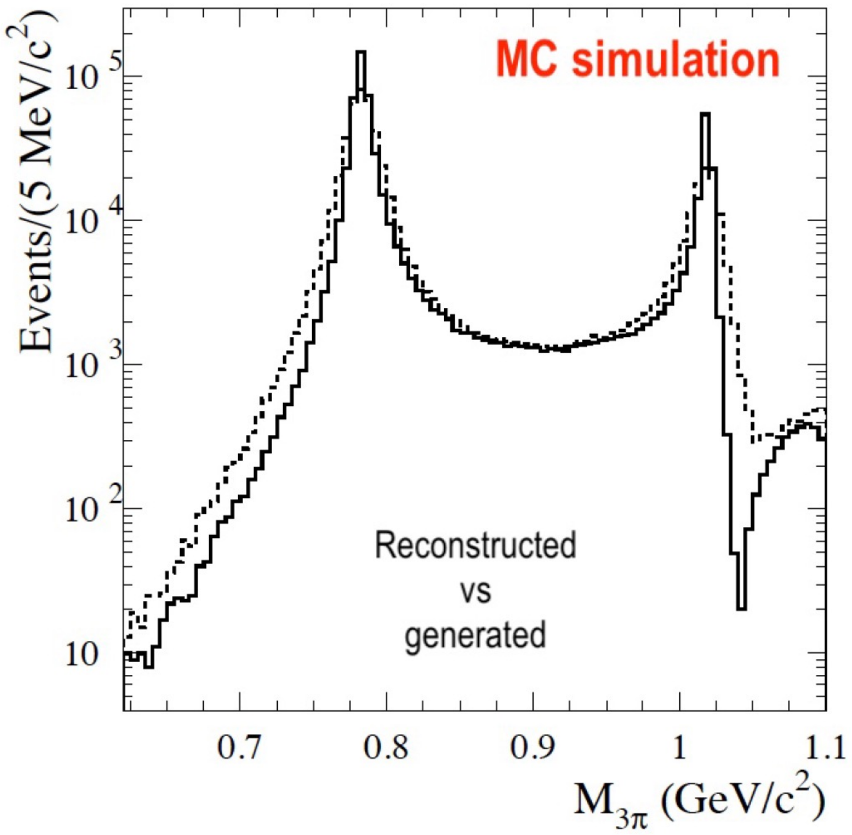

The ω and ϕ widths are well known

$\Longrightarrow$ use data to correct the simulated resolution function

Tails of the resolution depend on the χ^2 cut applied in selecting events:

$\Longrightarrow$ try more than one cut value

Fit to the $\pi^+\pi^-\pi^0$ mass spectrum

preliminary

The mass spectrum fitted with VDM model including

$\omega(782) + \omega(1420) + \omega(1680) + \phi(1020)$ resonances

$\omega(782)$ and ϕ widths fixed to PDG average

$+$ the rare $\rho(770) \to 3\pi$ decay

For $\chi^2 < 20$ (nominal fit) the mass spectrum is well described by introducing a Gaussian smearing of parameters

$\sigma_s = 1.5 \pm 0.2$ MeV

$m_\omega - m_{PDG} = 0.042 \pm 0.055$ MeV

$m_\phi - m_{PDG} = 0.095 \pm 0.084$ MeV

For $\chi^2 < 40$ (cross check): additional Lorentzian smearing required to describe tails $fraction = 0.7 \pm 0.2\,\%; \quad \gamma = 63 \pm 35$ GeV

consistent results for all other parameters

The data spectrum cannot be adequately described with $\mathcal{B}(\rho \to 3\pi) \equiv 0$

Fits to the $\pi^+\pi^-\pi^0$ mass spectrum ($\chi^2 < 40$)

preliminary

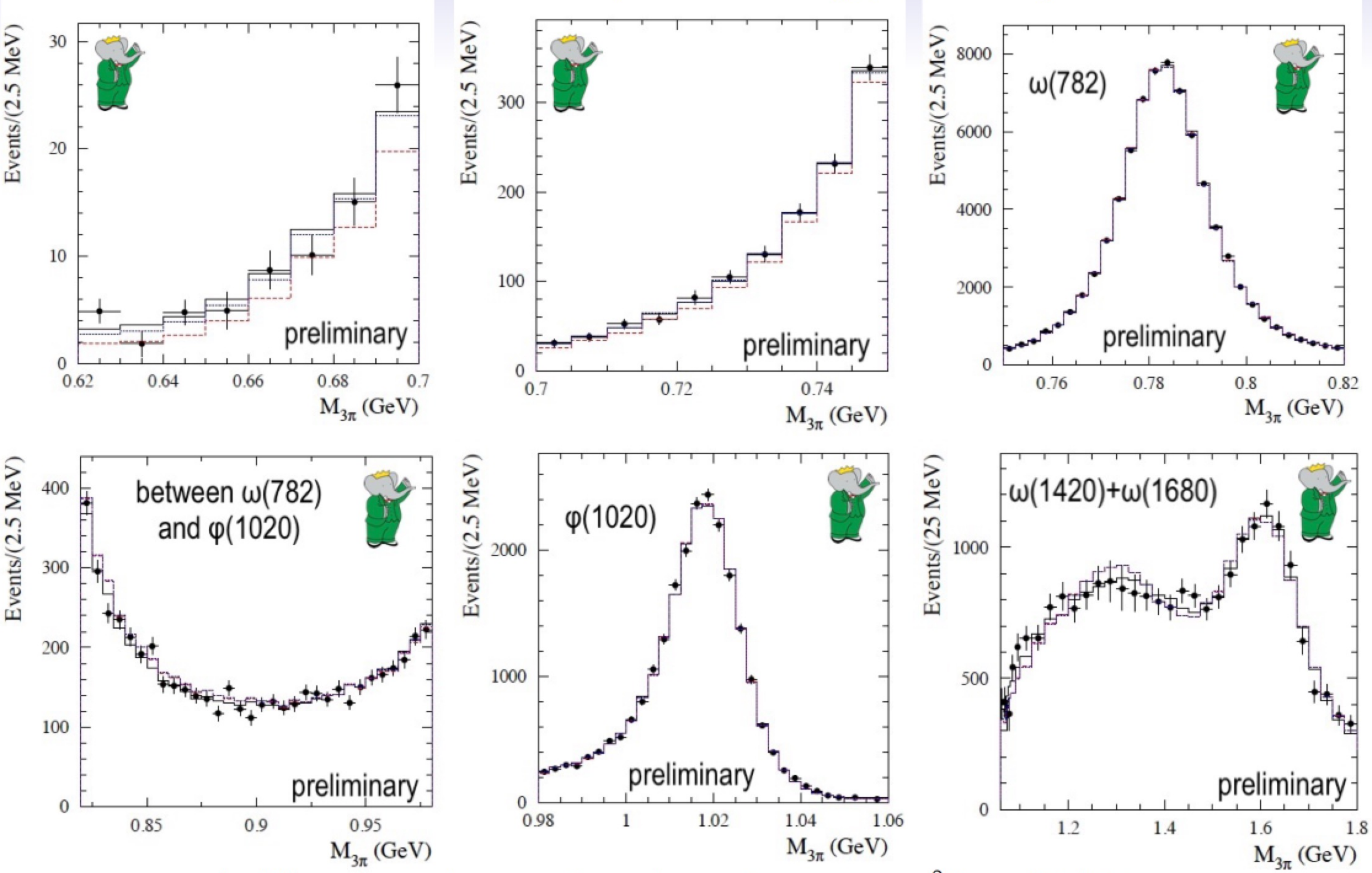

(solid):	Lorentzian smearing and $\rho \to 3\pi$	$\chi^2/\nu = 136/127$
(dash):	No Lorentzian smearing and no $\rho \to 3\pi$	$\chi^2/\nu = 201/131$
(dot):	Lorentzian smearing and no $\rho \to 3\pi$	$\chi^2/\nu = 180/129$

Fit results on resonance parameters

preliminary

For $\omega(782)$ and $\phi(1020)$ the products $\Gamma_{ee} \times \mathcal{B}_{3\pi}$ are in reasonable agreement with world average values:

$$\Gamma(\omega \to e^+e^-) \cdot \mathcal{B}(\omega \to \pi^+\pi^-\pi^0) = (0.5698 \pm 0.0031 \pm 0.0082)\ \mathrm{keV}$$

world average: $(0.557 \pm 0.011)\ \mathrm{keV}$

$$\Gamma(\phi \to e^+e^-) \cdot \mathcal{B}(\phi \to \pi^+\pi^-\pi^0) = (0.1841 \pm 0.0021 \pm 0.0080)\ \mathrm{keV}$$

world average: $(0.1925 \pm 0.0043)\ \mathrm{keV}$

The rare decay $\rho \to \pi^+\pi^-\pi^0$ is observed with significance greater than 6σ

the value and the relative phase wrt to the $\omega(782)$ amplitude are in agreement with the only previous measurement by SND

SND: Phys.Rev.D 63,07002 (2001)

$$\mathcal{B}(\rho \to \pi^+\pi^-\pi^0) = (0.88 \pm 0.23 \pm 0.30) \times 10^{-4}$$

SND: $(1.01^{+0.54}_{-0.34} \pm 0.34) \times 10^{-4}$

$$\phi_\rho - \phi_\omega = -(99 \pm 9 \pm 15)^o$$

SND: $-(135^{+17}_{-13} \pm 9)^o$

$e^+e^- \to \pi^+\pi^-\pi^0$ cross section below 1.1 GeV

preliminary

The parameters of the smearing function determined in the VDM fit are used to correct the simulated resolution function

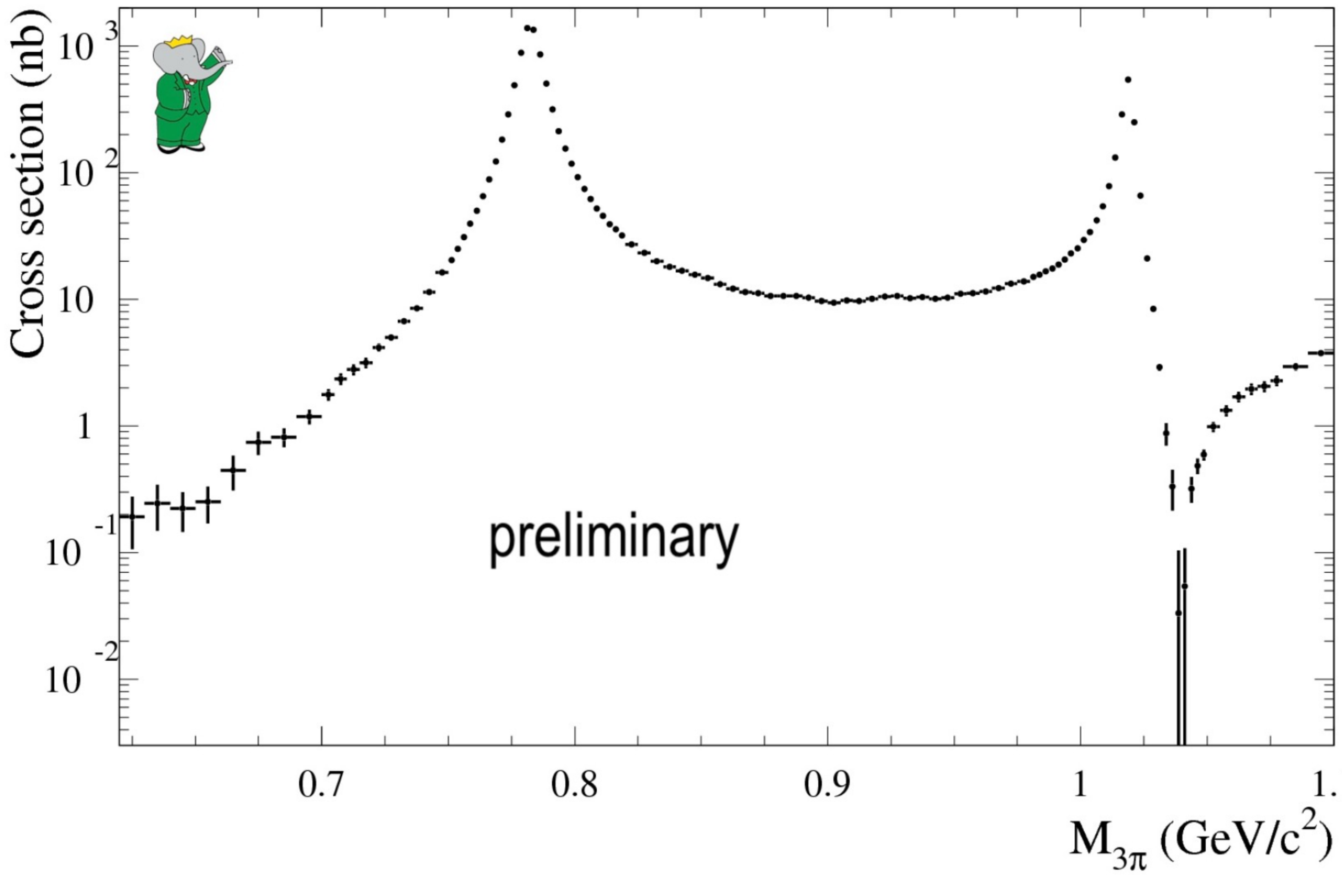

The unfolding is performed using the IDS (iterative dynamically stabilized) method (B. Malaescu, arXiv:0907.3791)

Systematic uncertainty at $\omega(782)$ and $\phi(1020)$ peak $\approx$1.3%

$e^+e^- \to \pi^+\pi^-\pi^0$ cross section below 1.1 GeV: comparison with previous measurements

preliminary

SND: Phys.Rev.D 68,052006 (2003)

CMD-2: Phys.Lett.B 578,285 (2004)

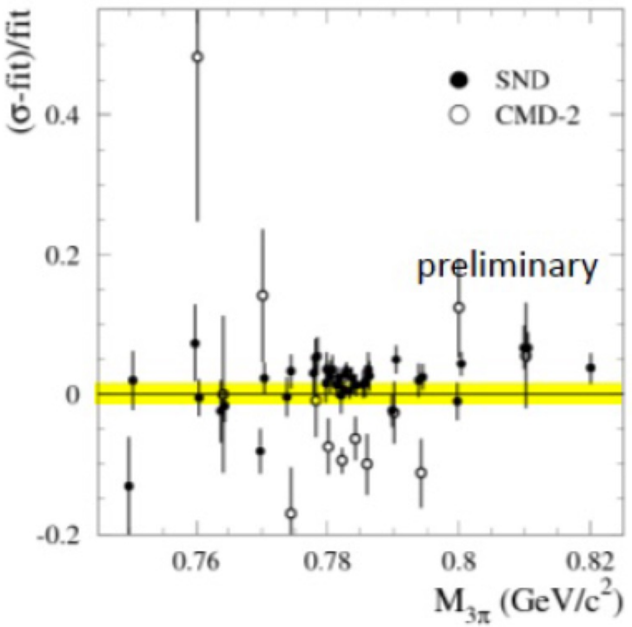

SND-*BABAR* difference $\simeq$ 2%
below syst. (3.4% SND, 1.4% *BABAR*)

CMD-2 (1.8% stat and 1.3% syst) is $\simeq$ 7% smaller than *BABAR*
$\approx 2.7\sigma$ difference

SND: Phys.Rev.D 63,072002 (2001)

CMD-2: Phys.Lett.B 642,203 (2006)

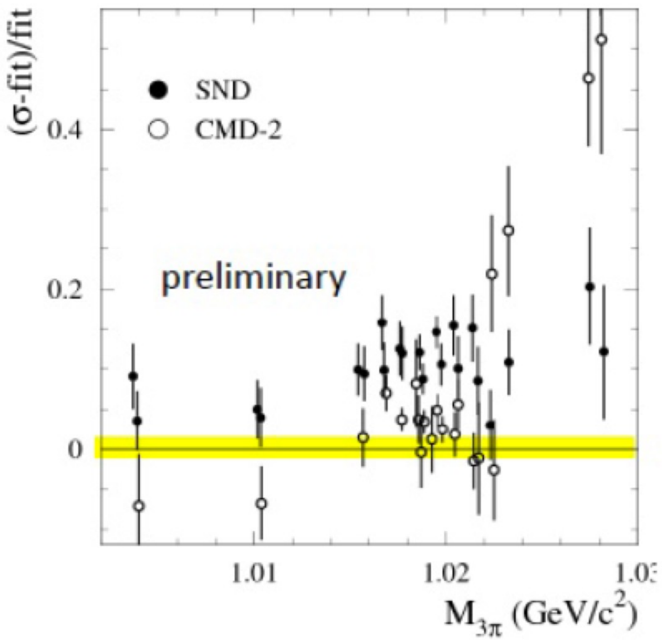

SND-*BABAR* difference $\simeq$ 11%
syst: 5% (SND); 1.4% (*BABAR*)

CMD-2-*BABAR* difference $\simeq$ 3%
syst: 2.5% (CMD-2); 1.4% (*BABAR*)

$e^+e^- \to \pi^+\pi^-\pi^0$ cross section above 1.1 GeV

preliminary

No smearing is needed above 1.1 GeV. Syst. uncertainty: $4 \div 15\%$ dominated by background subtraction

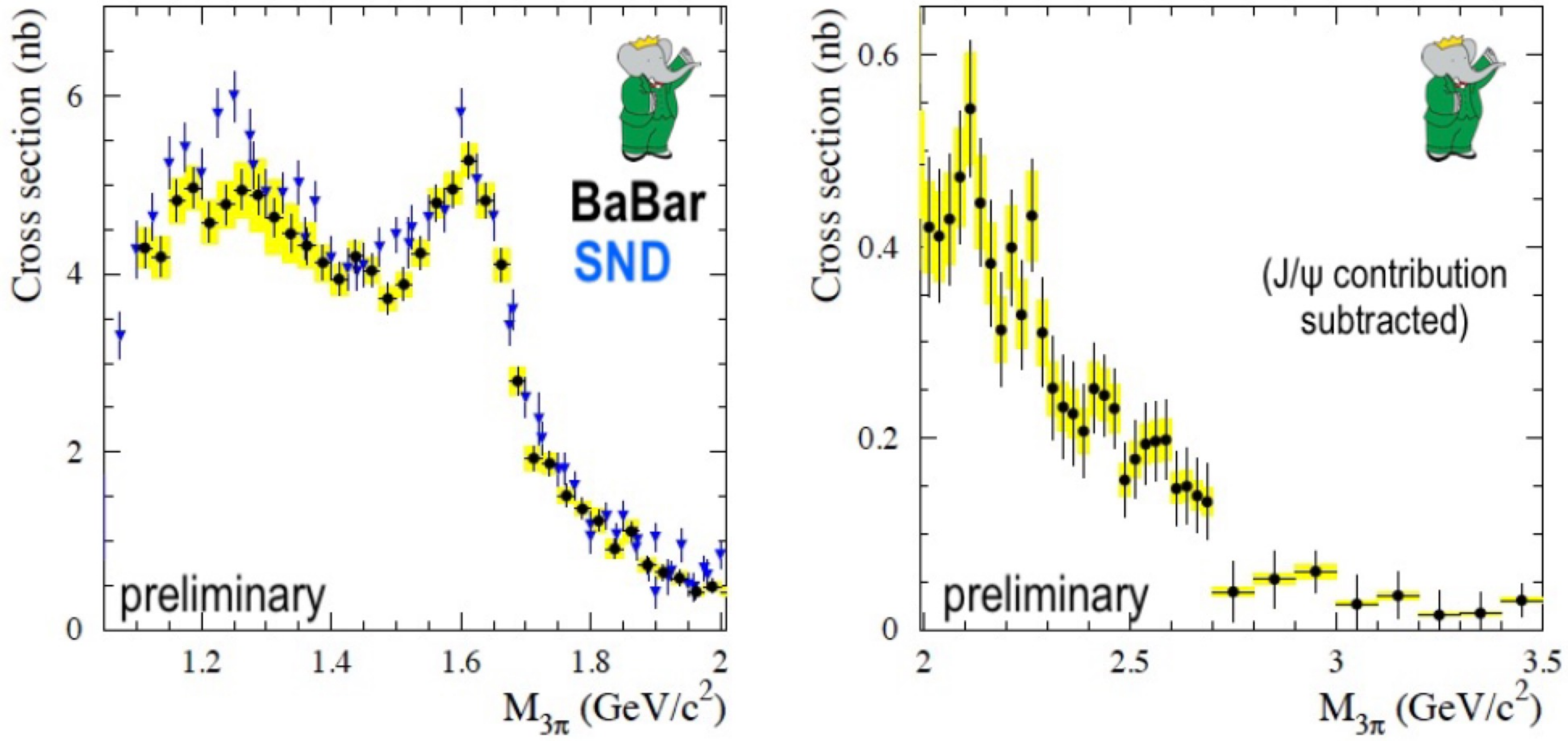

Significant localized differences around 1.25 GeV and 1.5 GeV between *BABAR* and SND (Eur.Phys.J. C 80, 993 (2020))

Impact on $a_\mu^{3\pi}$

preliminary

$M_{3\pi}$ GeV/c^2		$a_\mu^{3\pi} \times 10^{10}$
0.62–1.10		$42.91 \pm 0.14 \pm 0.55 \pm 0.09$
1.10–2.00		$2.95 \pm 0.03 \pm 0.16$
< 2.00	preliminary	$45.86 \pm 0.14 \pm 0.58$
< 1.80[A]		$46.21 \pm 0.40 \pm 1.40$
< 1.97[B]		46.74 ± 0.94
< 2[C]		44.32 ± 1.48

[A] M. Davier, A. Hoecker, B. Malaescu and Z. Zhang, Eur.Phys.J. C 80, 241 (2020)
[B] A. Keshavarzi, D. Nomura and T. Teubner, Phys.Rev.D 101, 014029 (2020)
[C] F. Jegerlehner, Springer Tracts Mod. Phys. 274, 1 (2017)

The value of $a_\mu^{3\pi}$ calculated using the preliminary $e^+e^- \to \pi^+\pi^-\pi^0$ cross-section is in reasonable agreement with earlier calculations

the error on this contribution is reduced by a factor ≈ 2

$e^+e^- \to \pi^+\pi^-4\pi^0$ and $\pi^+\pi^-3\pi^0\eta$ (first measurement)

preliminary

Events with 2 oppositely charged tracks, one γ_{ISR} photon candidate, 3 photon pairs with $m_{\gamma\gamma}$ compatible with π^0 and a 4-th photon pair

Signal events selected based on $\chi^2 < 70$; background from χ^2 sidebands

some additional cuts to reduce background

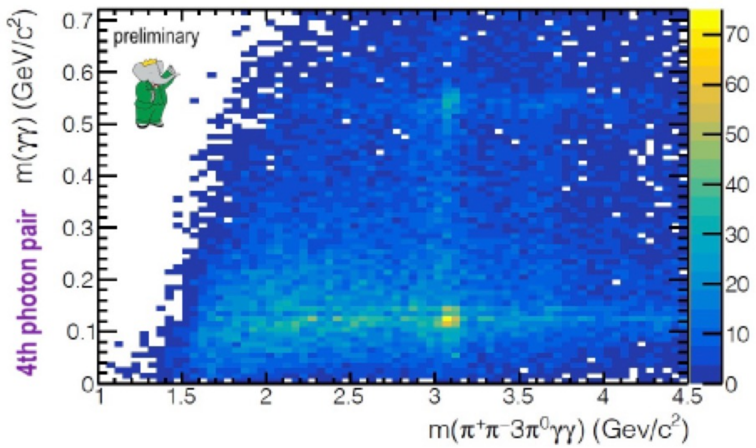

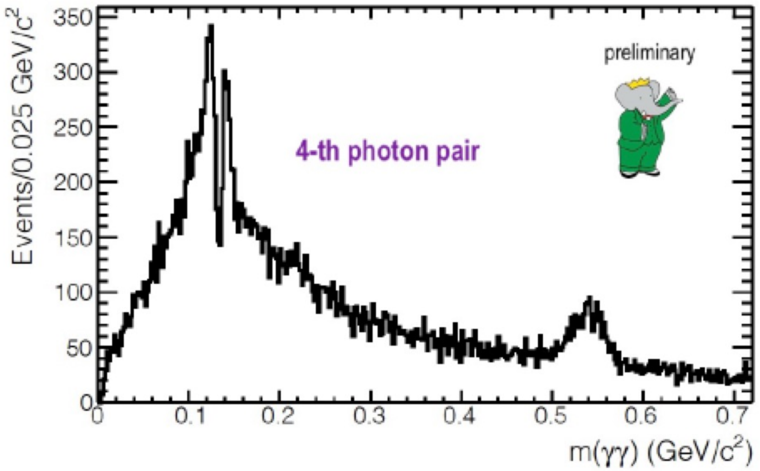

Fit the 4-th photon pair invariant mass distribution in bins of $m(\pi^+\pi^-3\pi^0\gamma\gamma)$ to determine the $\pi^+\pi^-4\pi^0$ and $\pi^+\pi^-3\pi^0\eta$ yields to determine cross sections

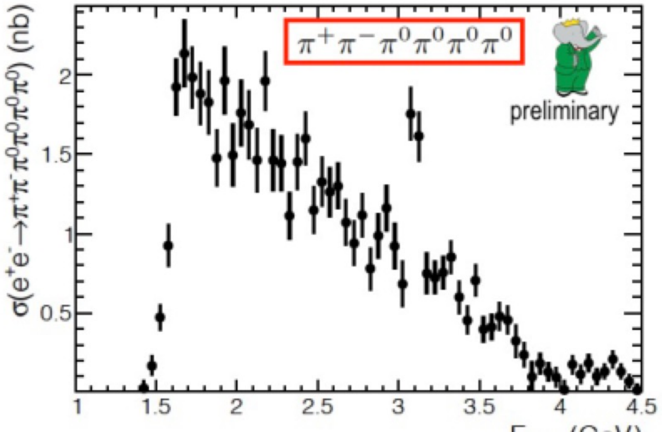

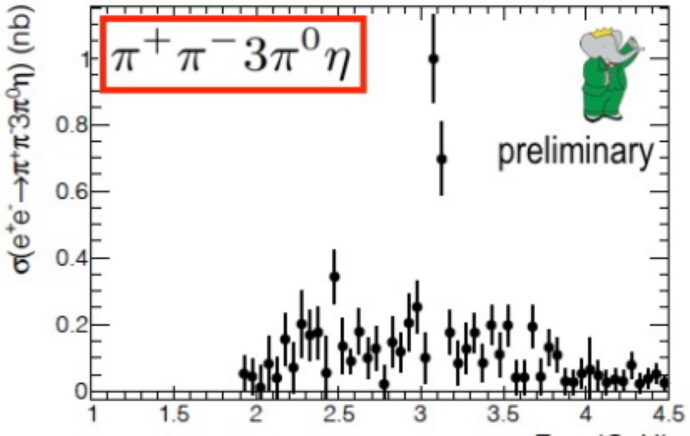

Substructures in $e^+e^- \to \pi^+\pi^-4\pi^0$

preliminary

Intermediate states:

$\pi^+\pi^-\pi^0\eta$ $\omega 3\pi^0$, $(\rho\pi)3\pi^0$

(possibly $\rho^+\rho^-2\pi^0$ above 2.9 GeV)

Sum of intermediate states seem to saturate the observed cross section

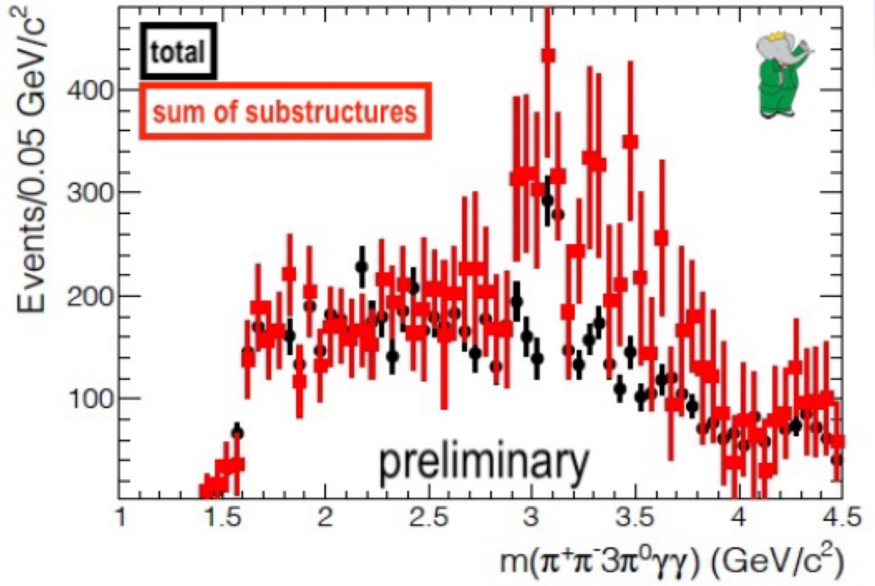

Below 2 GeV agreement with SND and CMD-2 measurements of $\pi^+\pi^-\pi^0\eta$ and $\omega\eta$:

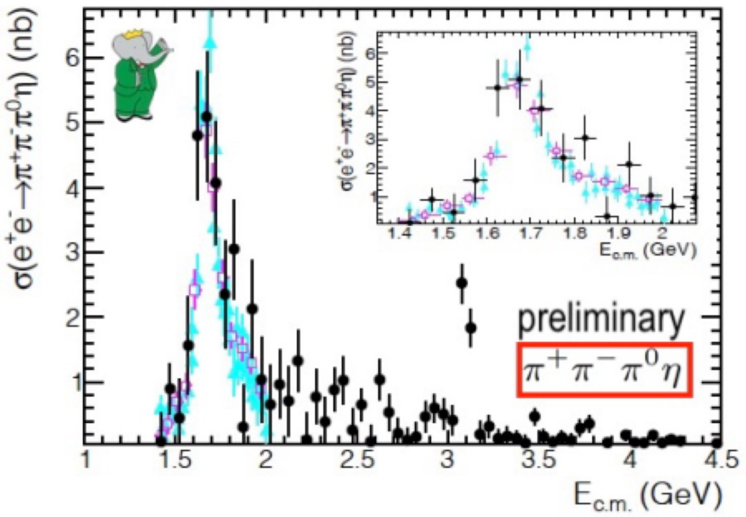

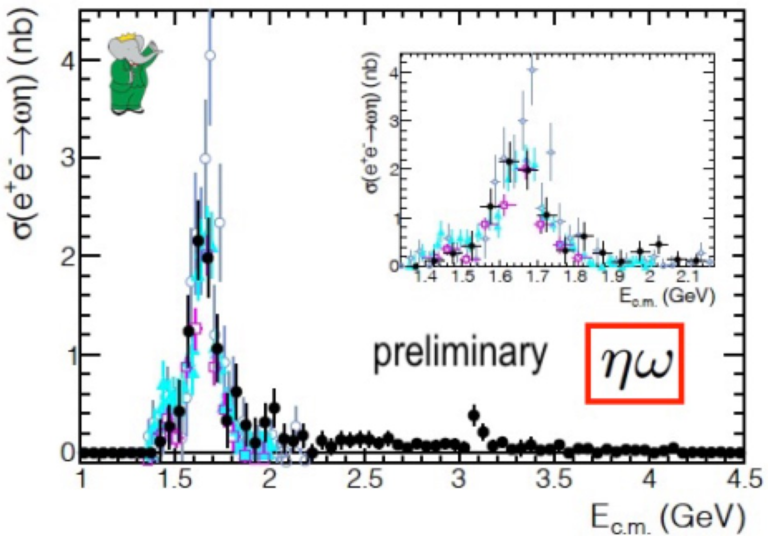

$e^+e^- \to \pi^+\pi^-4\pi^0$ and $\pi^+\pi^-3\pi^0\eta$: charmonium

preliminary

preliminary

Measured Quantity	Measured Value (eV)	J/ψ or $\psi(2S)$ Branching Fraction (10^{-3}) Calculated, this work	PDG [28]
$\Gamma_{ee}^{J/\psi}\cdot\mathcal{B}_{J/\psi\to\pi^+\pi^-\pi^0\pi^0\pi^0\pi^0}$	35.8±4.4±5.4	6.5±0.8±1.0	no entry
$\Gamma_{ee}^{J/\psi}\cdot\mathcal{B}_{J/\psi\to\eta\pi^+\pi^-\pi^0}\cdot\mathcal{B}_{\eta\to\pi^0\pi^0\pi^0}$	21.1±1.7±3.2	11.9±0.9±2.3	no entry
$\Gamma_{ee}^{J/\psi}\cdot\mathcal{B}_{J/\psi\to\omega\eta}\cdot\mathcal{B}_{\omega\to\pi^+\pi^-\pi^0}\cdot\mathcal{B}_{\eta\to\pi^0\pi^0\pi^0}$	4.9±2.1±0.7	3.0±1.3±0.5	1.74±0.20
$\Gamma_{ee}^{J/\psi}\cdot\mathcal{B}_{J/\psi\to\omega\pi^0\pi^0\pi^0}\cdot\mathcal{B}_{\omega\to\pi^+\pi^-\pi^0}$	9.4±2.3±1.5	1.9±0.5±0.3	no entry
$\Gamma_{ee}^{J/\psi}\cdot\mathcal{B}_{J/\psi\to\pi^+\pi^-\pi^0\pi^0\pi^0\eta}\cdot\mathcal{B}_{\eta\to\gamma\gamma}$	10.6±1.6±1.6	4.9±0.8±0.8	no entry
$\Gamma_{ee}^{\psi(2S)}\cdot\mathcal{B}_{\psi(2S)\to\pi^+\pi^-\pi^0\pi^0\pi^0\pi^0}$	3.3±2.3±0.5	1.4±1.0±0.2	no entry
$\Gamma_{ee}^{\psi(2S)}\cdot\mathcal{B}_{\psi(2S)\to\eta\pi^+\pi^-\pi^0}\cdot\mathcal{B}_{\eta\to\pi^0\pi^0\pi^0}$	<3.0 at 90% C.L.	<3.5 at 90% C.L.	no entry
$\Gamma_{ee}^{\psi(2S)}\cdot\mathcal{B}_{\psi(2S)\to\omega\eta}\cdot\mathcal{B}_{\omega\to\pi^+\pi^-\pi^0}\cdot\mathcal{B}_{\eta\to\pi^0\pi^0\pi^0}$	<1.1 at 90% C.L.	<1.4 at 90% C.L.	<0.11 at 90% C.L.
$\Gamma_{ee}^{\psi(2S)}\cdot\mathcal{B}_{\psi(2S)\to\omega\pi^0\pi^0\pi^0}\cdot\mathcal{B}_{\omega\to\pi^+\pi^-\pi^0}$	<1.6 at 90% C.L.	<0.8 at 90% C.L.	no entry
$\Gamma_{ee}^{\psi(2S)}\cdot\mathcal{B}_{\psi(2S)\to\pi^+\pi^-\pi^0\pi^0\pi^0\eta}\cdot\mathcal{B}_{\eta\to\gamma\gamma}$	<1.9 at 90% C.L.	<2.0 at 90% C.L.	no entry

Phys.Rev.D 103, 092001 (2021)

$e^+e^- \to 2(\pi^+\pi^-)3\pi^0$ and $2(\pi^+\pi^-)2\pi^0\eta$ (first measurement)

Events with 4 oppositely charged tracks, one γ_{ISR} photon candidate, 2 photon pairs with $m_{\gamma\gamma}$ compatible with π^0 and a 3-rd photon pair

Signal events selected based on $\chi^2 < 50$; background from χ^2 sidebands

some additional cuts to reduce background

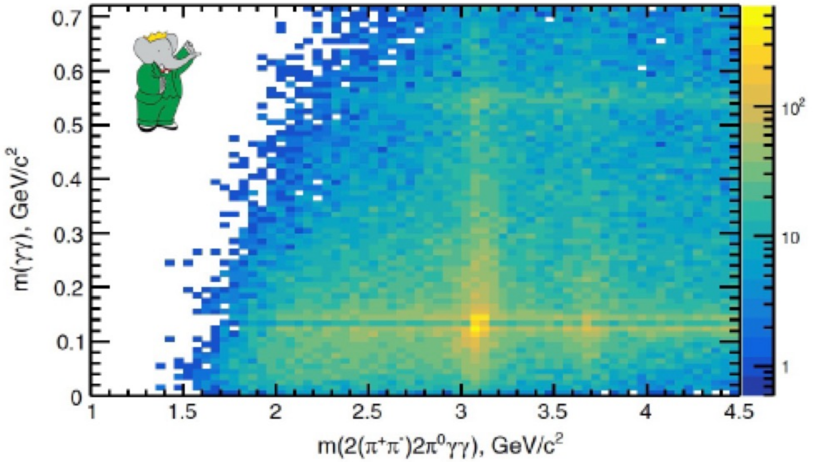

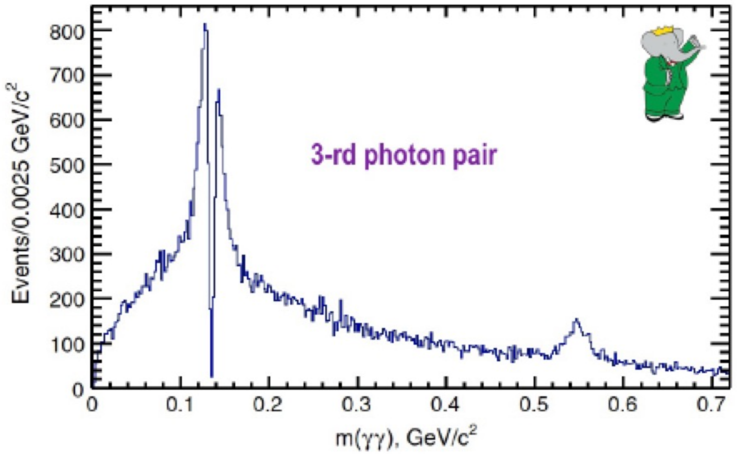

Fit the 3-rd photon pair mass distribution in bins of $m(2(\pi^+\pi^-)2\pi^0\gamma\gamma)$ to determine the $2(\pi^+\pi^-)3\pi^0$ and $2(\pi^+\pi^-)2\pi^0\eta$ yields to determine cross sections

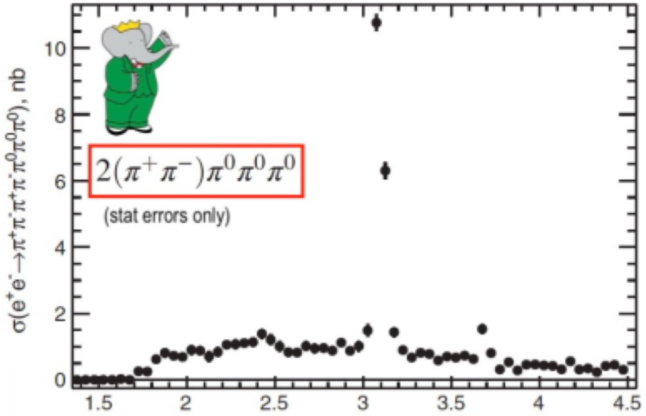

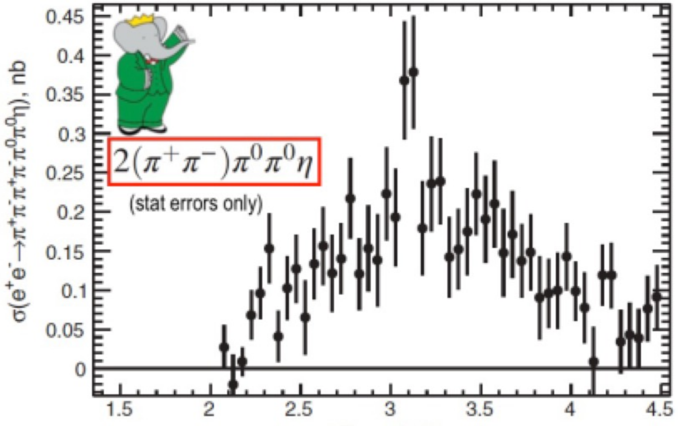

Phys.Rev.D 103, 092001 (2021)

Substructures in $e^+e^- \to 2(\pi^+\pi^-)3\pi^0$

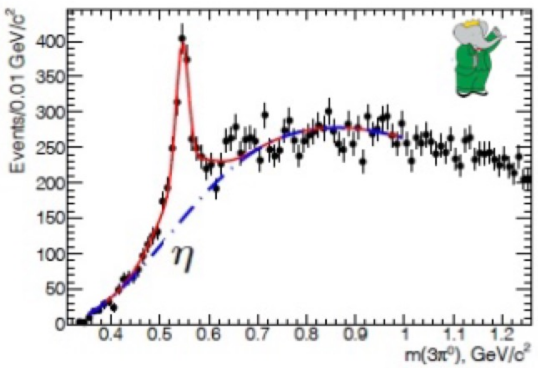

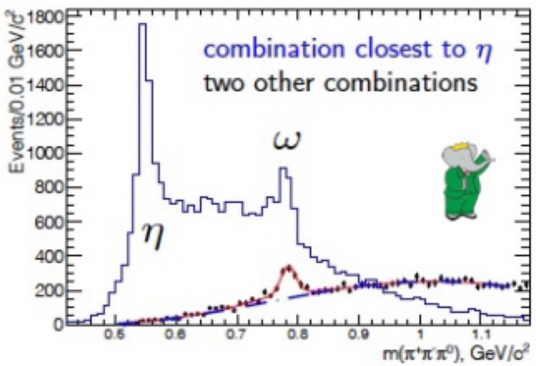

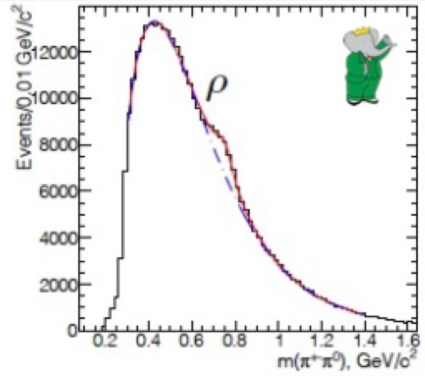

$e^+e^- \to \eta 2(\pi^+\pi^-)$

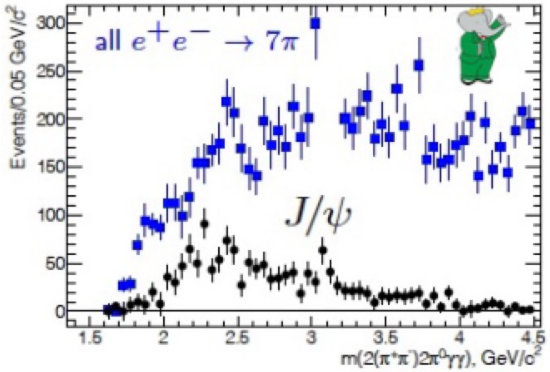

$e^+e^- \to \omega\pi^0\eta$

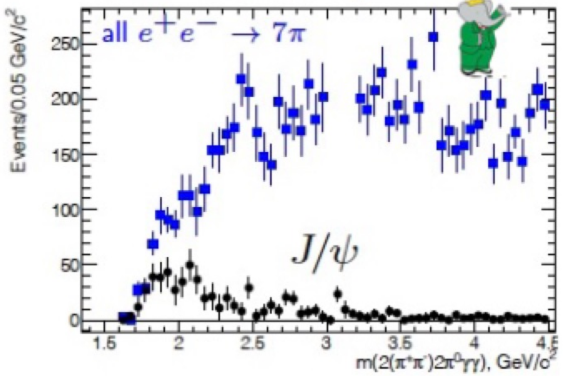

$\rho(770)^\pm\pi^\mp\pi^+\pi^-\pi^0\pi^0$

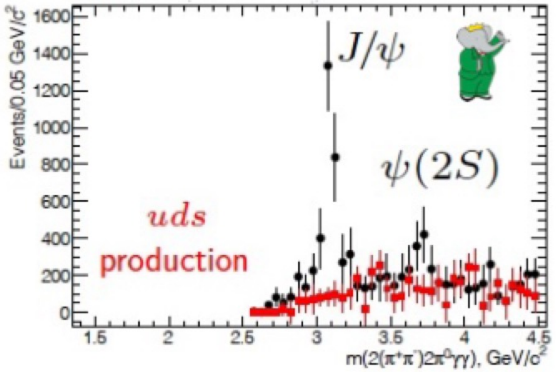

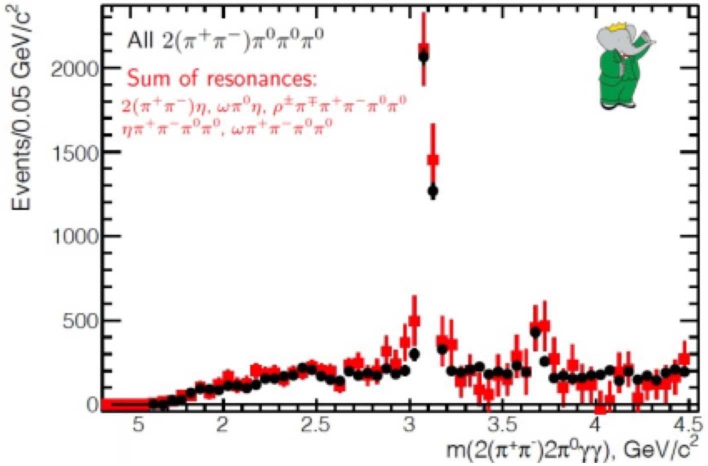

(not shown: $\eta\pi^+\pi^-2\pi^0$, $\omega\pi^+\pi^-2\pi^0$)

No significant evidence for intermediate states other than $2(\pi^+\pi^-)\eta$, $\omega\pi^0\eta$, $\rho^\pm\pi^\mp\pi^+\pi^-2\pi^0$, $\eta\pi^+\pi^-2\pi^0$, $\omega\pi^+\pi^-2\pi^0$

$e^+e^- \to 2(\pi^+\pi^-)3\pi^0$ and $2(\pi^+\pi^-)2\pi^0\eta$: charmonium

Phys.Rev.D 103, 092001 (2021)

		J/ψ or $\psi(2S)$ branching fraction (10^{-3})	
Measured quantity	Measured value (eV)	Calculated, this work	PDG [22]
$\Gamma_{ee}^{J/\psi} \cdot \mathcal{B}_{J/\psi\to\pi^+\pi^-\pi^+\pi^-\pi^0\pi^0\pi^0}$	$345.0 \pm 10.0 \pm 50.0$	$62.0 \pm 2.0 \pm 9.0$	No entry
$\Gamma_{ee}^{J/\psi} \cdot \mathcal{B}_{J/\psi\to\omega\pi^+\pi^-\pi^0\pi^0} \cdot \mathcal{B}_{\omega\to\pi^+\pi^-\pi^0}$	$165.0 \pm 9.0 \pm 25.0$	$33.0 \pm 2.0 \pm 5.0$	No entry
$\Gamma_{ee}^{J/\psi} \cdot \mathcal{B}_{J/\psi\to\eta\pi^+\pi^-\pi^0\pi^0} \cdot \mathcal{B}_{\eta\to\pi^+\pi^-\pi^0}$	$6.0 \pm 4.0 \pm 1.0$	$4.8 \pm 3.2 \pm 0.8$	2.3 ± 0.5
$\Gamma_{ee}^{J/\psi} \cdot \mathcal{B}_{J/\psi\to\pi^+\pi^-\pi^+\pi^-\eta} \cdot \mathcal{B}_{\eta\to\pi^0\pi^0\pi^0}$	$5.6 \pm 2.6 \pm 0.8$	$2.6 \pm 1.2 \pm 0.5$	2.26 ± 0.28
$\Gamma_{ee}^{J/\psi} \cdot \mathcal{B}_{J/\psi\to\rho^\pm\pi^\mp\pi^+\pi^-\pi^0\pi^0}$	$155.0 \pm 26.0 \pm 36.0$	$28.0 \pm 4.7 \pm 6.6$	No entry
$\Gamma_{ee}^{J/\psi} \cdot \mathcal{B}_{J/\psi\to\rho^+\rho^-\pi^+\pi^-\pi^0}$	$32.0 \pm 13.0 \pm 15.0$	$5.7 \pm 2.4 \pm 2.7$	No entry
$\Gamma_{ee}^{J/\psi} \cdot \mathcal{B}_{J/\psi\to\pi^+\pi^-\pi^+\pi^-\pi^0\pi^0\eta} \cdot \mathcal{B}_{\eta\to\gamma\gamma}$	$9.1 \pm 2.6 \pm 1.4$	$4.2 \pm 1.2 \pm 0.6$	No entry
$\Gamma_{ee}^{\psi(2S)} \cdot \mathcal{B}_{\psi(2S)\to\pi^+\pi^-\pi^+\pi^-\pi^0\pi^0\pi^0}$	$33.0 \pm 5.0 \pm 5.0$	$14.0 \pm 2.0 \pm 2.0$	No entry
$\Gamma_{ee}^{\psi(2S)} \cdot \mathcal{B}_{\psi(2S)\to J/\psi\pi^0\pi^0} \cdot \mathcal{B}_{J/\psi\to\pi^+\pi^-\pi^+\pi^-\pi^0}$	$14.8 \pm 2.6 \pm 2.2$	$34.7 \pm 6.1 \pm 5.2$	33.7 ± 2.6
$\Gamma_{ee}^{\psi(2S)} \cdot \mathcal{B}_{\psi(2S)\to J/\psi\pi^+\pi^-} \cdot \mathcal{B}_{J/\psi\to\pi^+\pi^-\pi^0\pi^0\pi^0}$	$19.2 \pm 4.5 \pm 3.2$	$23.8 \pm 5.6 \pm 3.6$	27.1 ± 2.9
$\Gamma_{ee}^{\psi(2S)} \cdot \mathcal{B}_{\psi(2S)\to\omega\pi^+\pi^-\pi^0\pi^0} \cdot \mathcal{B}_{\omega\to\pi^+\pi^-\pi^0}$	$18.0 \pm 4.0 \pm 3.0$	$8.7 \pm 1.9 \pm 1.5$	No entry
$\Gamma_{ee}^{\psi(2S)} \cdot \mathcal{B}_{\psi(2S)\to\pi^+\pi^-\pi^+\pi^-\pi^0\pi^0\eta} \cdot \mathcal{B}_{\eta\to\gamma\gamma}$	<1.9 at 90% C.L.	<2.0 at 90% C.L.	No entry
$\Gamma_{ee}^{\psi(2S)} \cdot \mathcal{B}_{\psi(2S)\to\pi^+\pi^-\pi^+\pi^-\eta} \cdot \mathcal{B}_{\eta\to\pi^0\pi^0\pi^0}$	<2.3 at 90% C.L.	<2.4 at 90% C.L.	1.2 ± 0.6

Conclusions

New measurement of the $e^+e^- \to \pi^+\pi^-\pi^0$ cross section

preliminary

- based on the entire BABAR dataset
- measured in the range $0.62 \div 3.5$ GeV
- 1.3% systematic uncertainty near the maxima of $\omega(782)$ and $\phi(1020)$
- the error on the leading order contribution to muon magnetic anomaly from $e^+e^- \to \pi^+\pi^-\pi^0$ ($E < 2$ GeV) reduced by a factor ≈ 2

First measurements of $e^+e^- \to \pi^+\pi^- 4\pi^0$ and $e^+e^- \to \pi^+\pi^- 3\pi^0\eta$ cross sections

preliminary

- $e^+e^- \to \pi^+\pi^- 4\pi^0$ cross section seem to be saturated by intermediate states: $\pi^+\pi^-\pi^0\eta$, $\omega 3\pi^0$, $(\rho\pi)3\pi^0$ and possibly $\rho^+\rho^- 2\pi^0$ intermediate states
- new J/ψ and $\psi(2S)$ decay modes

First measurements of $e^+e^- \to 2(\pi^+\pi^-)3\pi^0$ and $e^+e^- \to 2(\pi^+\pi^-)2\pi^0\eta$ cross sections

Phys.Rev.D 103, 092001 (2021)

- $e^+e^- \to 2(\pi^+\pi^-)3\pi^0$ cross section seem to be saturated by intermediate states: $2(\pi^+\pi^-)\eta$, $\omega\pi^0\eta$, $\rho^\pm\pi^\mp\pi^+\pi^- 2\pi^0$, $\eta\pi^+\pi^- 2\pi^0$, $\omega\pi^+\pi^- 2\pi^0$
- new J/ψ and $\psi(2S)$ decay modes


BACKUP

$a_\mu = \frac{1}{2}(g-2)_\mu$ precision test of SM

SM prediction for muons: $a_\mu = a_\mu^{QED} + a_\mu^{EW} + a_\mu^{hadr}$

absolute value dominated by $a_\mu^{QED} + a_\mu^{EW}$

ERROR dominated by a_μ^{hadr}: not calculable perturbatively

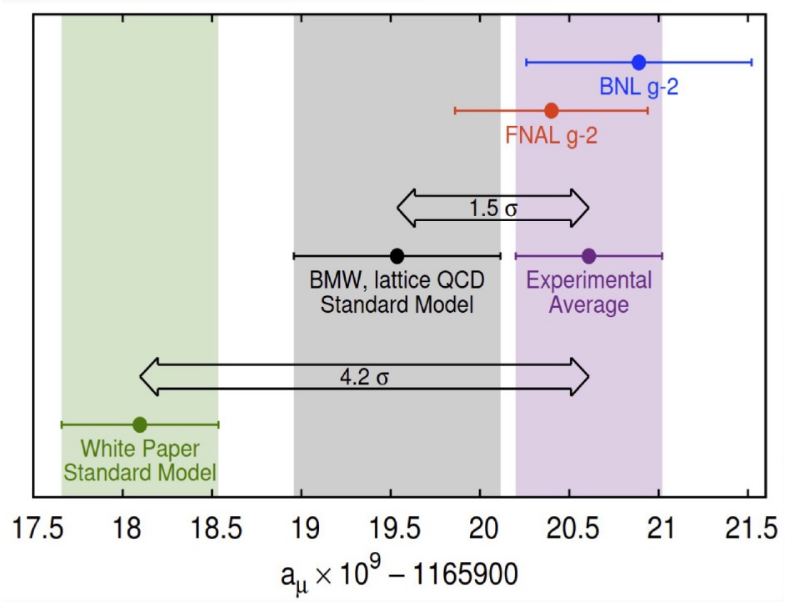

4.2 σ (WP/SM) or 1.5 σ (LQCD/SM)

a_μ^{hadr}: LQCD or data-driven dispersive approach

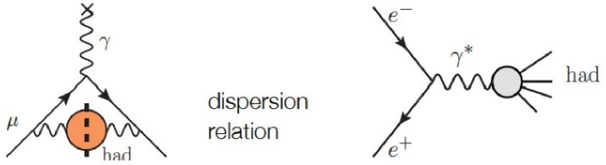

$K(s)$: analytically known kernel function

$$a_\mu^{\mathrm{had,LO}} = \frac{\alpha^2(0)}{3\pi^2} \int_{4m_\pi^2}^{\infty} ds \, \frac{K(s)}{s} R(s)$$

$$R(s) = \frac{\sigma(e^+e^- \to \mathrm{hadrons})}{\sigma(e^+e^- \to \mu^+\mu^-)}$$ experimental input

relies on hadronic cross section measurements

Largest contribution to the integral from hadronic cross section at low energies

For $\sqrt{s} \lesssim 2\ GeV$ finite number of final states contribute:

$\sigma(e^+e^- \to \mathrm{hadrons})$ can be obtained as sum of all exclusive cross sections

The *BABAR* experiment

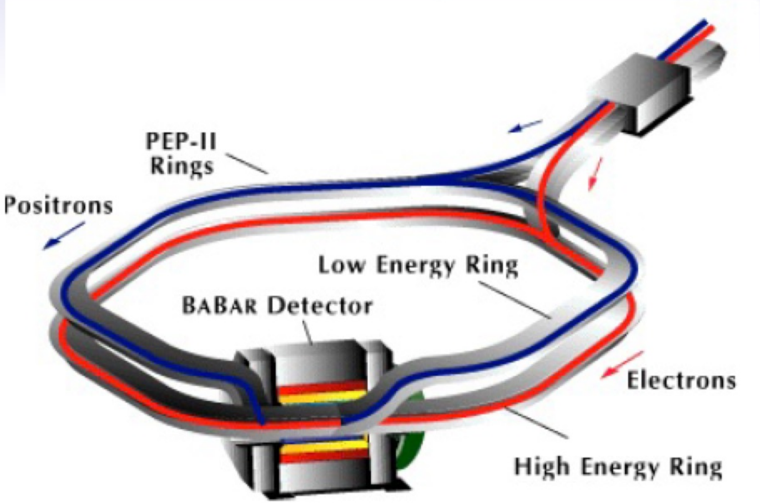

PEP-II asymmetric e^+e^- collider operating at center of mass energies near the $\Upsilon(4S)$ (for most of the time)

$$\sqrt{s} = 10.58\,\mathrm{GeV}/c^2$$

General-purpose detector

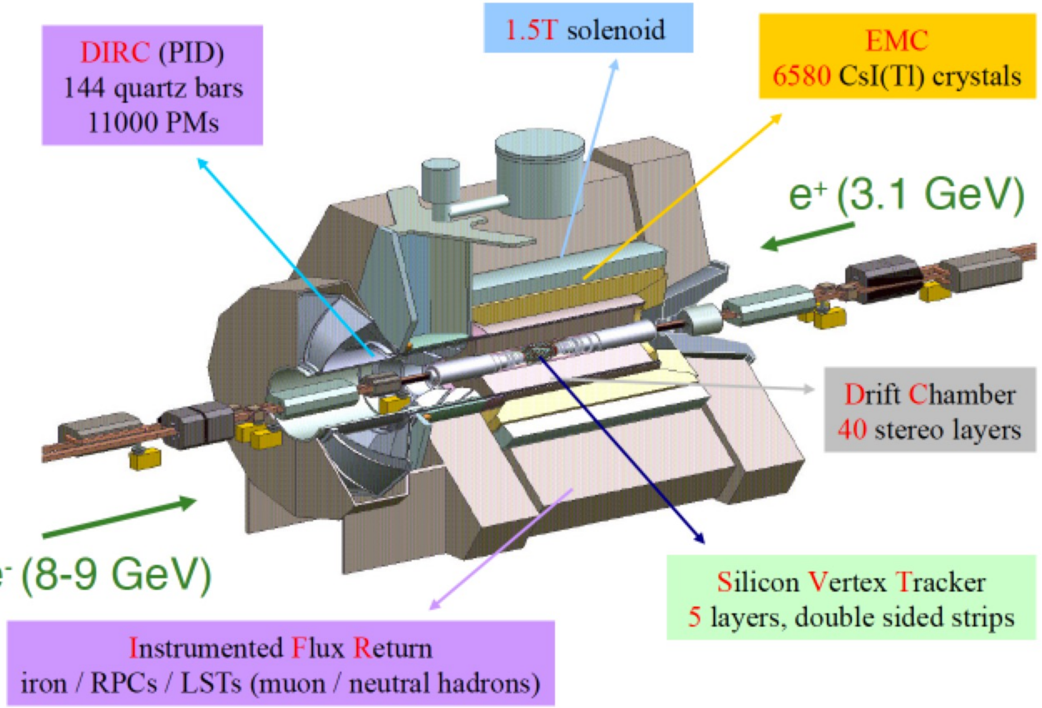

Asymmetric detector:

$$-0.9 < \cos\theta^* < 0.85$$

wrt electron beam

excellent performance:

- vertexing
- tracking
- PID
- calorimeter

Data samples

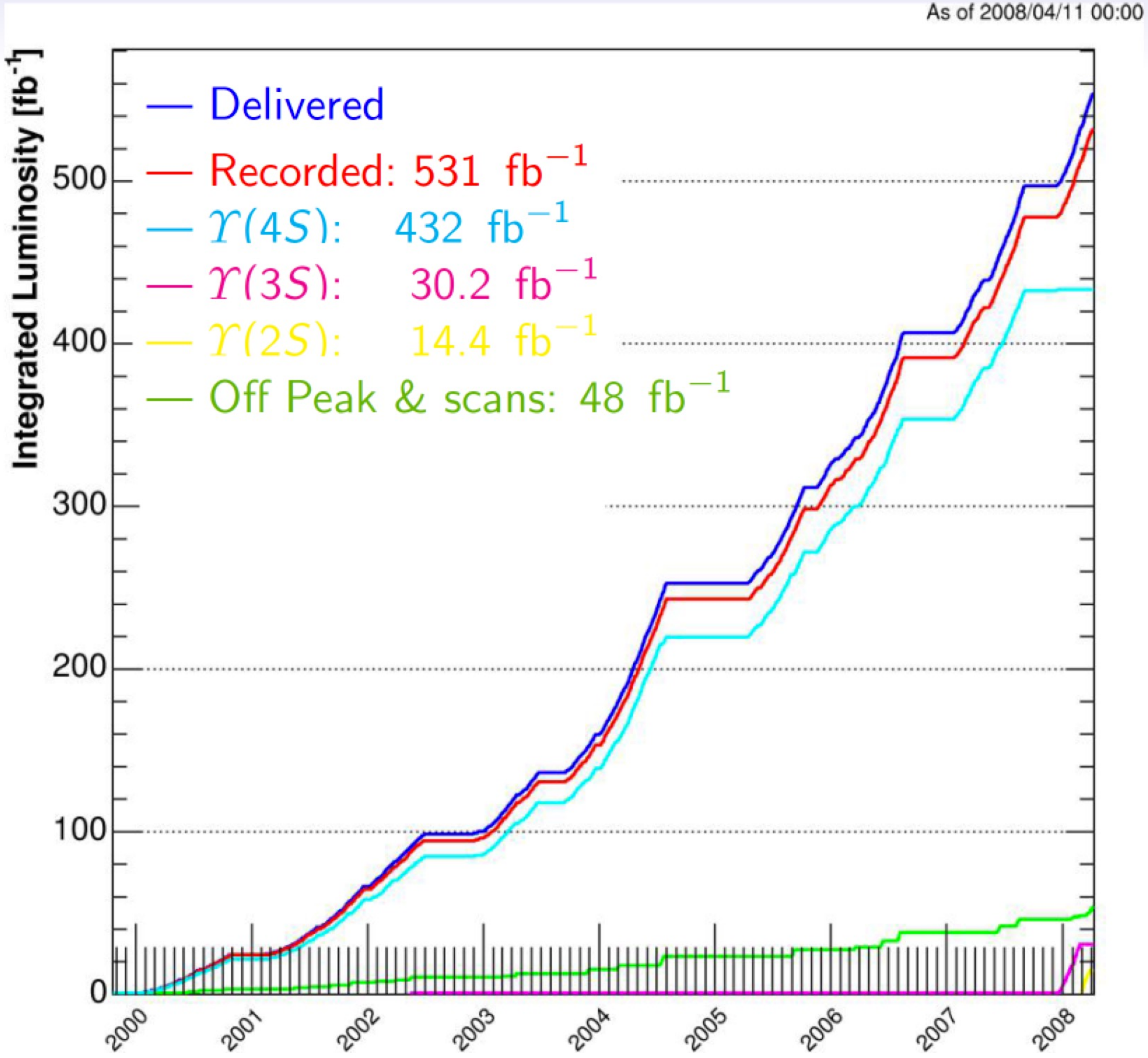

Light hadrons cross sections measured by *BABAR*

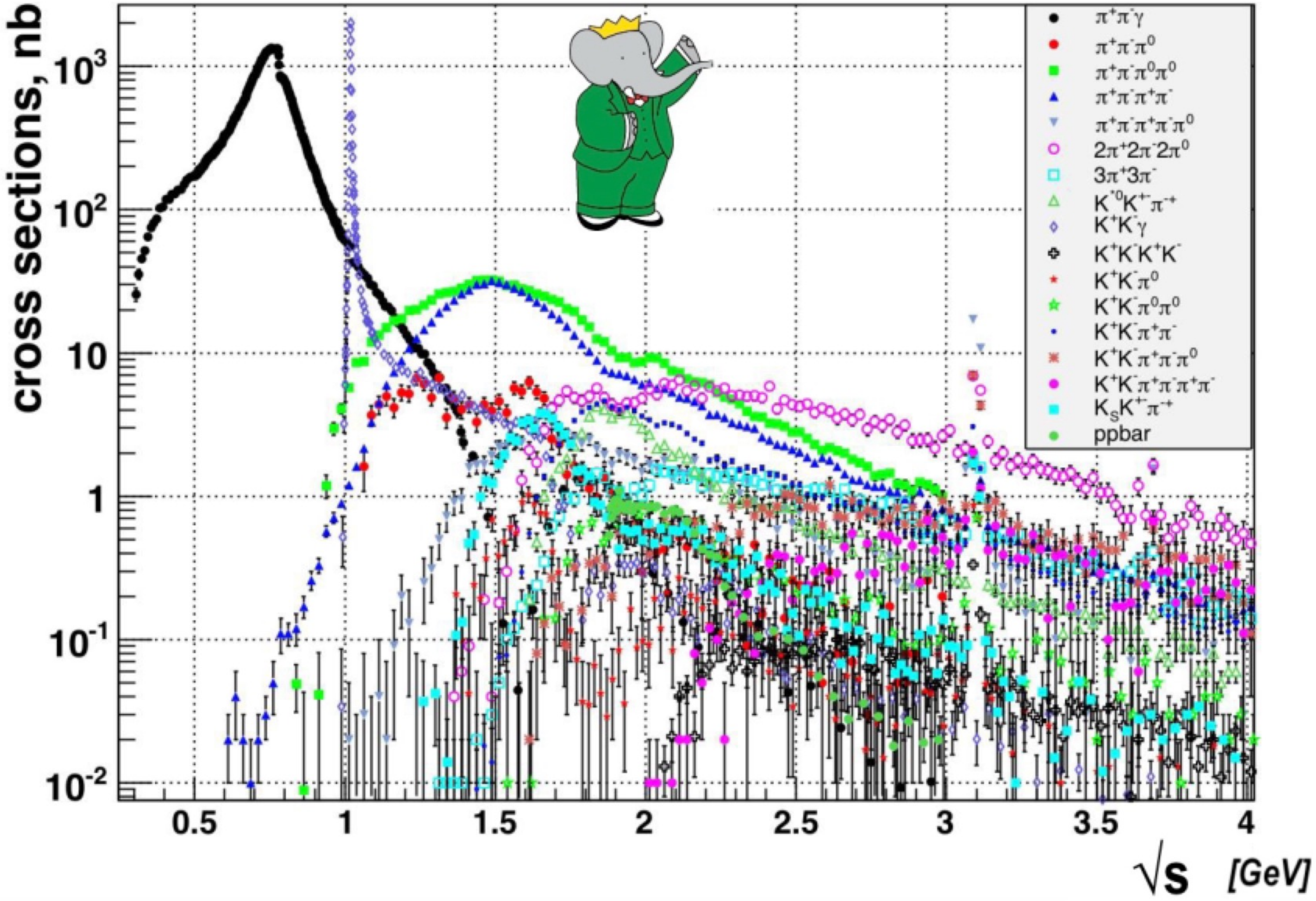

Substructures in $e^+e^- \to \pi^+\pi^-4\pi^0$